Detailed Characterization of Electron Plasma Waves Produced by Stimulated Raman Scattering

N. Renard, C. Labaune, H. A. Baldis,* B. S. Bauer,† B. Quesnel, E. Schifano, and A. Michard
Laboratoire pour l'Utilisation des Lasers Intenses, Ecole Polytechnique, Centre National de la Recherche Scientifique, 91128 Palaiseau cedex, France

W. Seka
Laboratory for Laser Energetics, University of Rochester, Rochester, New York 14627

K. G. Estabrook
Lawrence Livermore National Laboratory, Livermore, California 94550
(Received 8 July 1996)

Time-resolved spectra and location of electron plasma waves (EPW) produced by stimulated Raman scattering in back and in side directions have been measured using Thomson scattering of a short wavelength probe beam. Significant Raman sidescattering was observed for angles as large as 40° from the laser axis. The Raman growth is larger and starts earlier in the front part of the density profile than at the summit. Simultaneous measurements at multiple places in the plasma provided an indication of the coherence length of the EPW. [S0031-9007(96)01552-9]

PACS numbers: 52.35.Fp, 52.35.Mw, 52.40.Nk, 52.50.Jm

Stimulated Raman scattering (SRS) is a parametric instability in which an incident electromagnetic wave $(\omega_0, \vec{k}_0)$ decays into an electron plasma wave (EPW) $(\omega_{\mathrm{epw}}, \vec{k}_{\mathrm{epw}})$ and a scattered electromagnetic wave (EM) $(\omega_{\mathrm{SRS}}, \vec{k}_{\mathrm{SRS}})$ [1–5]. The production of hot electrons associated with this instability, as well as the loss or the redistribution of the incident laser energy in millimeter scale plasmas, can have detrimental effects on fusion. Many experiments have concentrated on the observation of the EM backscattered SRS wave as this instability has the highest growth rate in backward direction [6,7]. The SRS sidescattered light has been observed previously only from large planar plasmas [8], where refraction and absorption of this light may have modified the scattering measurements and the angular distribution in a non-negligible way.

In the present experiment, the electron plasma waves, corresponding to different Raman geometries, have been probed by Thomson scattering [9] and analyzed by a single diagnostic. An array of three different interaction beams has provided the characterization of EPW associated with Raman sidescattering over a large range of angles with no ambiguity. This unique setup allows a perfect relative calibration between the different waves which are observed with negligible modification by absorption or refraction effects. Significant Raman sidescattering was observed for angles as large as 40° from the laser axis. The measurements are resolved in time, wavelength, space, and wave number. Two unexpected results are that the Raman starts to grow late in the laser pulse and is maximum in the front part of the density profile.

The experiment was performed using the six beams of the LULI laser facility. Figure 1 shows the experimental setup. All beams were in the horizontal plane. Two of the 600 ps FWHM Gaussian beams, converted to the second harmonic ($\lambda = 527$ nm), arrived from opposite directions at $t = 0$ onto the thin foil to produce the plasma. Random phase plates (RPP) [10] were used on each one of the beams to obtain plasma conditions as reproducible as possible. Three independent laser beams were used, one at a time, to produce the interaction with the preformed plasma. The paper reports on electron plasma waves produced by these beams. The wavelength of all the interaction beams was 1.053 μm, and they arrived on target 1.72 ns after the plasma producing beams. Using a focusing lens, with an aperture of $f/6$, and an RPP, with 2 mm elements, each interaction beam was focused into a 320 μm diameter focal spot, 1.5 mm focal depth, producing a maximum intensity at best focus of 10^{14} W/cm^2.

Targets were mass-limited freestanding, $(C_8H_8)_n$ foils of 400 μm diameter and 1.5 μm thickness. The targets burned through towards the end of the primary plasma producing beams. The orientation of the targets was chosen perpendicular to the interaction beam in order to present an axially symmetric long-scale-length plasma to the interaction beam. The density profile had an

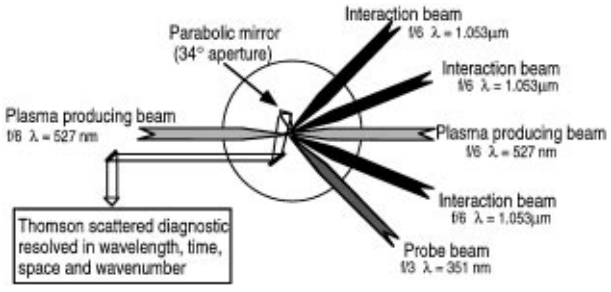

FIG. 1. Experimental setup.

approximately inverse parabolic shape along the laser axis with a scale length of ~1 mm, and was flat over a distance of ~400 μm in the transverse direction. The maximum electron density on the axis decreased between $0.25n_c$ and $0.08n_c$ during the interaction pulse due to plasma expansion (n_c is the critical density for 1.053 μm laser light, $n_c = 1.1 \times 10^{21}$ cm^{-3}). The electron temperature had been measured using thermal Thomson scattering in the absence of interaction beam [11], and is ~0.5 keV at $t = 1.7$ ns. 2D hydrodynamics simulations show that the plasma was heated during interaction to ~0.7 keV.

The plasma was probed by an uv laser beam ($\lambda = 351$ nm). The probe beam was focused onto the plasma with an $f/3$ lens combined with an RPP with elongated elements (0.1×0.9) mm^2, producing a line focus of 100 μm $\times$ 1 mm along the axis of the interaction beam. The volume of plasma irradiated by the probe beam contained most of the focal waist of the interaction beam thus allowing simultaneous Thomson scattering from all along the interaction beam within the plasma. The Thomson scattered light was collected with an off-axis, 34° aperture, parabolic mirror, of high quality, which was part of the optical system imaging the focal region onto the entrance slit of a spectrometer. The spectrometer was coupled with a streak camera with three entrance slits, allowing the simultaneous registration of three time-resolved spectra emitted by three different regions of plasma along the density profile [12]. Each spectrum supplies information on the EPW produced in a well defined region of plasma, with dimensions (20×40) μm. This system provides absolute correlation between EPW growing at well defined positions in the plasma within 40 μm. Time resolution was 45 ps, and spectra resolution was 5 Å. The wave numbers of the plasma waves were selected by angularly resolving the scattered light with 5° aperture slits placed at the exit of the chamber. Each of the three interaction beams, having a different direction with respect to the Thomson scattering diagnostic, gave angularly selected scattered light corresponding to EPW associated with different Raman geometries. Thomson scattered light from ion acoustic waves (IAW) associated with stimulated Brillouin scattering (SBS) was analyzed as well.

Figure 2 shows a typical time-resolved spectrum of Thomson scattered light from electron plasma waves. These particular data correspond to waves located at the top of the density profile. The first component in time, with wavelength ~421 nm, corresponds to the scattering of the probe beam on the electron plasma waves produced by the two plasmon decay instability ($3\omega - 1/2\omega = 5/2\omega$). This shows the presence, early in the pulse, of densities close to quarter-critical density. The second part of the spectrum starts around the peak of the interaction beam and exhibits wavelengths evolving from 401 to 376 nm. This component lasts ~300 ps and corresponds to the scattering of the probe beam on the

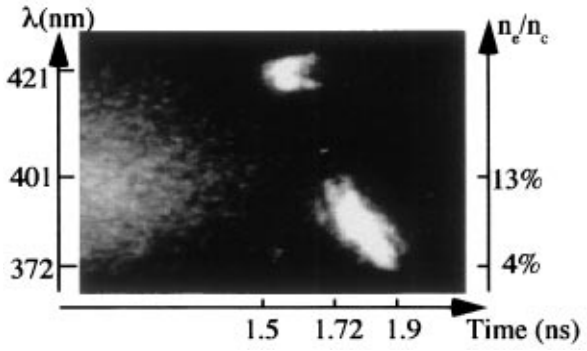

FIG. 2. Time-resolved spectrum of Thomson scattered light from electron plasma waves located at the top of the density profile.

electron plasma waves produced by backward stimulated Raman scattering. By using the relationship between the frequency of the Thomson scattered light (ω_{TS}), the EPW frequencies (ω_{EPW}), and the probe frequency (ω_{probe}), $\omega_{\mathrm{TS}} = \omega_{\mathrm{probe}} - \omega_{\mathrm{EPW}}$, the plasma densities at which the EPW have been produced can be deduced from the scattered wavelengths by the following relation: $n_e/n_c = 9(1 - \lambda_{\mathrm{probe}}/\lambda_{\mathrm{TS}})^2$. This was obtained by neglecting the Bohm-Gross correction to the frequency of the plasma waves, which is insignificant for the electron temperature encountered in these experiments. The spectrum for EPW shown in Fig. 2 corresponds to plasma densities evolving between 13% and 4% of the critical density. A large gap between 25% and 13% of critical density, with no Raman emission, is clearly observed.

Time-resolved spectra of the Thomson scattered light from EPW associated with backward SRS growing at eight different positions in the plasma along the laser axis are shown in Fig. 3. Consecutive regions are separated by 110 μm, the laser beam is coming from the right, and these spectra have been recorded using three laser shots, each providing three spectra, with an overlap

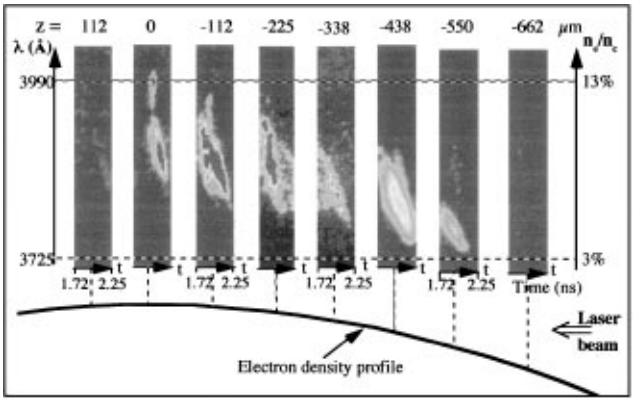

FIG. 3. Time-resolved spectra of the Thomson scattered light from electron plasma waves associated with stimulated Raman backscattering probed at different positions along the laser axis.

of one slit between shots. To keep the signals within the dynamic range of the streak camera, different attenuations have been used depending on the observed region of plasma. The left edge of each frame corresponds to time $t = 1.72$ ns, which is the peak of the interaction pulse. All the spectra exhibit the behavior which has been previously described for Fig. 2. Electron densities deduced from these frames provide an excellent measurement of the shape of the density profile as a function of time [13]. The important features of these spectra are the relative intensities of the scattered light as a function of position inside the density profile and the comparison of the temporal evolution of the signals between different frames. The scattered light starts earlier in the front part of the density profile than at the summit. The largest delay is for the rear part of the plasma, where the signal is also the weakest. The brightest emission is located ~ 200 μm from the summit towards the laser beam. We observe a slight shift of the position of this maximum towards the summit as time increases. The total spatial extent of the region of activity of EPW is around 700 μm with relative intensities between the maximum and minimum scattered light of ~ 10. Some correlation between the structures observed in consecutive frames, for the same laser shot, was observed only if the distance between the regions of plasma was smaller than 200 μm. This length gives an estimate of the coherence length of the EPW.

The variations of the level of the EPW associated with stimulated Raman scattering have been studied as a function of the angle of the Raman decay. We define θ as the angle between the pump beam and the electromagnetic scattered wave ($\theta = 180°$ is direct backscatter). Figure 4 shows time-resolved spectra of the Thomson scattered light from EPW associated with various Raman angles between 180° and 90°, which correspond, respectively, to back and sidescatter. Studies of the emission as a function of the position have shown that the location of the brightest emission moves towards the summit of the density profile when the Raman angle decreases. The frames presented in Fig. 4 correspond to the position of maximum emission for each geometry.

The angular diagram of the total scattered light is obtained by integrating the time-resolved spectra and is shown in Fig. 5. Scattered intensities are normalized to the backscattered intensity. This diagram is peaked in the backward direction, as expected from the convective growth rate [5], and its aperture is larger than the beam aperture, indicating significant sidescattering for angles as large as 40° from the laser axis. Modeling of the level of density fluctuations associated with the EPW driven by SRS as a function of angle is ongoing work and will be published shortly.

The two new important results, which are the localization of EPW in the front part of the plasma relative to the interaction beam and the delayed start of the Raman emission, can be consistently explained by the interplay between stimulated Brillouin and Raman scattering during the first part of the laser pulse. These two instabilities can be considered as growing in isolated speckles produced by the RPP, in combination with the focusing lens, in the focal volume. Statistical theory of SBS in randomly distributed speckles [14,15] has been applied to this experiment [16], predicting fairly well the main observed features. SBS starts first to grow in speckles with intensity around 4 times the average laser intensity. Such speckles are in the regime of strong pump depletion which produces a shift of the maximum of density fluctuations towards the laser as they follow the intensity distribution. During this period of active SBS, SRS is inhibited either because of the ion fluctuations [17] which destroy the matching conditions, or because of pump depletion as

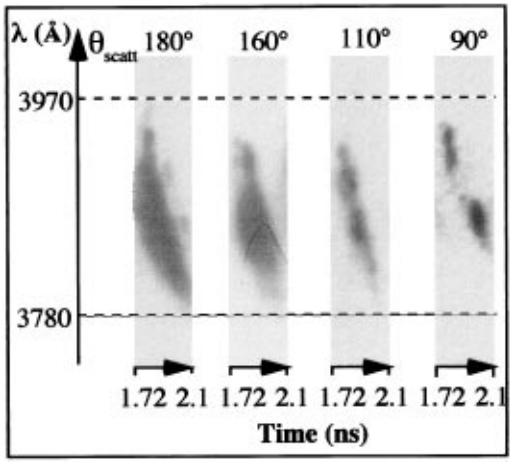

FIG. 4. Time-resolved spectra of Thomson scattered light from electron plasma waves associated with various stimulated Raman scattering decays.

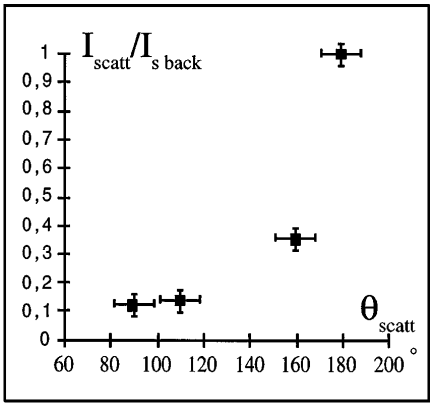

FIG. 5. Angular diagram of Thomson scattered light intensity from EPW associated with SRS as a function of the SRS angle (180° corresponds to backscattering). The scattered intensities have been normalized to the intensity obtained for backscattering.

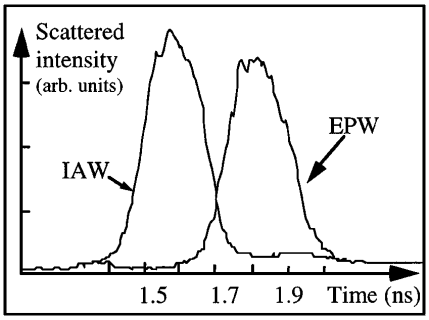

FIG. 6. Experimental temporal evolution of the ion acoustic waves associated with stimulated Brillouin scattering and of the electron plasma waves associated with stimulated Raman scattering.

the two instabilities are sharing the same pump and the same speckles. SRS starts to grow later in the laser pulse, when the SBS gain has been reduced mainly because of the drop of electron density. Observed temporal behaviors of IAW and EPW associated, respectively, with SBS and SRS, and located in the same region of plasma, are shown in Fig. 6. The waves clearly follow the temporal evolution described above, demonstrating the inhibition of SRS in the early part of the laser pulse. The location of SRS in the front part of the plasma, at the starting point, corresponds to the present location of the maximum of the laser intensity distribution which is due to a combination of pump depletion in SBS-active speckles and absorption of the overall laser beam. As SBS drops, the shift due to pump depletion decreases, and the region of activity of Raman moves towards the summit. The gap of Raman is a direct consequence of the delay of the Raman growth because of Brillouin. The maximum electron densities present at the time when Raman starts are around 13%. This gap is larger than most of the observations reported before [6,7].

In summary, direct measurements of the density fluctuations associated with electron plasma waves produced by stimulated Raman scattering show evidence of nonnegligible sidescattering processes. The angular diagram of the level of EPW is peaked in the backward direction, with an aspect ration of ~ 9 from backward (180°) to side (90°) directions. The application of the multiplexing technique provided, for the first time, a detailed correlation between EPW growing at different locations within the interaction region, indicating that the coherence length of the EPW is smaller than 200 μm. The location of EPW in the front part of the plasma can be explained by the laser intensity distribution which has been affected by the combined effects of pump depletion in the SBS active speckles and overall absorption. It is interesting to notice that although the conditions of this experiment are completely different from the ones described in Ref. [18], the interpretation of the Raman gap is based on the same physics.

The authors gratefully acknowledge valuable discussions with V. T. Tikhonchuk, the target fabrication of H. Timsit and C. Coulaud, and the laser group of LULI who made this experiment possible.

*Also at Lawrence Livermore National Laboratory, Livermore, California 94550.
†Present address: Department of Physics, University of Nevada, Reno, NV 89509.

[1] M. N. Rosenbluth, Phys. Rev. Lett. **29**, 565 (1972).
[2] M. N. Rosenbluth, R. B. White, and C. S. Liu, Phys. Rev. Lett. **31**, 1190 (1973).
[3] J. F. Drake, P. K. Kaw, Y. C. Lee, C. S. Liu, M. N. Rosenbluth, and G. Shmidt, Phys. Fluids **17**, 778 (1974).
[4] D. W. Forslund, J. M. Kindel, and E. L. Lindman, Phys. Fluids **18**, 1002 (1975).
[5] W. L. Kruer, *The Physics of Laser Plasma Interactions* (Addison-Wesley Publishing Company, Inc., Redwood City, CA, 1988); D. Pesme, *L'interaction laser-matière dans "La fusion thermonucléaire inertielle par laser,"* edited by R. Dautray and J. P. Watteau (Eyrolles, Paris, 1993); E. A. Williams and T. W. Johnston, Phys. Fluids B **1**, 188 (1989).
[6] H. A. Baldis, E. M. Campbell, and W. L. Kruer, in *Physics of Laser Plasma*, edited by A. Rubenchik and W. Witkowski (North-Holland, Amsterdam, 1991), p. 361–434; R. P. Drake, Laser Part. Beams **10**, 599 (1992).
[7] K. Tanaka *et al.*, Phys. Rev. Lett. **48**, 1179 (1982); D. W. Phillion *et al.*, Phys. Rev. Lett. **49**, 1405 (1982); C. L. Shepard *et al.*, Phys. Fluids B **1**, 1089 (1989); C. Labaune *et al.*, Phys. Fluids B **2**, 166 (1990).
[8] R. P. Drake *et al.*, Phys. Fluids **31**, 3130 (1988); R. P. Drake *et al.*, Phys. Rev. Lett. **53**, 1739 (1984).
[9] H. A. Baldis, D. M. Villeneuve, and C. J. Walsh, Can. J. Phys. **64**, 961 (1986).
[10] Y. Kato *et al.*, Phys. Rev. Lett. **53**, 1057 (1984).
[11] C. Labaune, H. A. Baldis, N. Renard, E. Schifano, S. Baton, A. Michard, W. Seka, R. E. Bahr, B. Bauer, K. Baker, and K. Estabrook, Phys. Rev. Lett. **75**, 248 (1995).
[12] H. A. Baldis and C. Labaune, Rev. Sci. Instrum. **67**, 451 (1996).
[13] W. Seka, R. S. Craxton, C. Labaune, H. A. Baldis, N. Renard, E. Schifano, and A. Michard, Bull. Am. Phys. Soc. **40**, 11 (1995); **40**, 1777 (1995).
[14] H. A. Rose and D. F. DuBois, Phys. Fluids B **5**, 590 (1993).
[15] H. A. Rose and D. F. DuBois, Phys. Rev. Lett. **72**, 2883 (1994); H. A. Rose, Phys. Plasmas **2**, 2216 (1995).
[16] V. T. Tikhonchuk, C. Labaune, and H. A. Baldis, Phys. Plasmas (to be published).
[17] W. Rozmus, A. A. Offenberger, and R. Fedosejevs, Phys. Fluids **26**, 1071 (1983); H. C. Barr and F. Chen, Phys. Fluids **30**, 1180 (1987); G. Bonnaud, Laser Part. Beams **5**, 101 (1987); H. A. Rose, D. F. DuBois, and B. Bezzerides, Phys. Rev. Lett. **58**, 2547 (1987); W. Rozmus, R. P. Sharpa, J. C. Samson, and W. Tighe, Phys. Fluids **30**, 2181 (1987).
[18] H. A. Baldis, P. E. Young, R. P. Drake, W. L. Kruer, K. Estabrook, E. A. Williams, and T. W. Johnson, Phys. Rev. Lett. **62**, 2829 (1989).